Physica 148A (1988) 343–355
North-Holland, Amsterdam

ELECTROMAGNETIC WAVE PROPAGATION IN QUASIPERIODICALLY STRATIFIED MEDIA

D. WÜRTZ*, T. SCHNEIDER and M.P. SOERENSEN**
IBM Research Division, Zurich Research Laboratory, 8803 Rüschlikon, Switzerland

Received 19 June 1987

We explore the wave number dependence of the transmission of electromagnetic waves in quasiperiodic dielectric multilayers. Using the transfer-matrix technique, we also establish the connection to the tight-binding Schrödinger problem. As an example, we consider a multilayer constructed according to the Fibonacci inflation rule. In contrast to the periodic case, we find a highly fragmented distribution of stop bands and self-similar structure in the wave number dependence of transmission.

1. Introduction

Recently, the one-dimensional Schrödinger equation with quasiperiodic potential evoked considerable interest[1–6]). This equation displays fragmented eigenvalue spectra because a quasiperiodic potential is intermediate between a random one, yielding exponentially localized wave functions[7]), and the periodic potentials, leading to energy bands and gaps. Moreover, the new ability to produce semiconductor heterostructures with control of each layer allows experimental realizations of these structures[8]). Here, the one-dimensional Schrödinger equation models the properties of the heterostructure perpendicular to the layers.

In this work, we explore a related problem, electromagnetic wave propagation in layered and quasiperiodic dielectric media. The regular counterpart, periodically stratified media, has a long history[9]) and many important applications, ranging from optical filters to reflectors, solid-state lasers and optical fibers[10]). In analogy to the Schrödinger problem, one expects quasiperiodic stratified media to represent an intermediate case between the periodic and

*Permanent address: Institut für Theoretische Physik, Universität Heidelberg, Philosophenweg 19, D-6900 Heidelberg, Fed. Rep. Germany.
**Permanent address: Laboratory of Applied Mathematical Physics, Technical University of Denmark, Building 303, DK-2800 Lyngby, Denmark.

random ones. To substantiate this expectation, we calculate the wave number dependence of the transmission coefficients for the periodic and quasiperiodic cases. We assume linear wave propagation and use transfer-matrix techniques to calculate the wave number dependence of the reflection and transmission coefficients. In the periodic case, we reproduce the well-known result, that for certain wave number or frequency bands almost total reflection or transmission can occur. In the Schrödinger problem, the reflection or stop bands correspond to the gaps. In the case of quasiperiodic stratified media, as an example, we consider multilayers made up of two materials arranged according to the Fibonacci inflation rule. In contrast to the periodic case, we find a highly fragmented distribution of stop bands and self-similar structure in the wave number dependence of the transmission. Similarly, the integrated density of states of the associated Schrödinger problem is also highly fragmented and exhibits scaling properties. For a large number of layers, fragmentation implies that any randomly chosen wave number will be in a stop band with probability one. Thus, high transmission occurs for very special wave numbers only.

The paper is organized as follows. In section 2, we sketch the formalism to calculate transmission and reflection, and establish the connection to the Schrödinger problem. The models for layers arranged periodically and quasiperiodically are presented in section 3. Here, we also discuss the numerical results and the scaling properties of transmission and integrated density of states of the associated Schrödinger problem in terms of a recursion relation for transfer matrices.

2. Formalism

Following the textbook of Born and Wolf[9]) we consider the propagation of a transverse electromagnetic wave through a stratified medium consisting of homogeneous layers. The stratification is assumed to be along the z-axis. The electric field of the wave is perpendicular to the plane of incidence, i.e., the yz-plane. Accordingly, the only non-vanishing component of the electric field $\boldsymbol{E}$ is the x-component E_x. The dielectric constant and the magnetic permeability are denoted by ε and μ, respectively. We assume non-magnetic materials where $\mu = 1$, and consider normal incidence. In this case, only the y-component H_y of the magnetic field $\boldsymbol{H}$ is different from zero. According to Maxwell's equations, it can be shown that within one layer, E_x and H_y are given by

$$E_x = U(z)\,\mathrm{e}^{-\mathrm{i}\omega t}\,, \quad H_y = V(z)\,\mathrm{e}^{-\mathrm{i}\omega t}\,; \tag{1}$$

t denotes the time, and ω is the frequency of the electromagnetic wave. The

two amplitudes $U(z)$ and $V(z)$ satisfy

$$\frac{\mathrm{d}U}{\mathrm{d}z} = \mathrm{i}k_0\mu V = \mathrm{i}k_0 V\ , \quad \frac{\mathrm{d}V}{\mathrm{d}z} = \mathrm{i}k_0\varepsilon U\ . \tag{2}$$

The wave number k_0 is given by $k_0 = \omega/c = 2\pi/\lambda_0$, where c is the vacuum velocity of light and λ_0 the associated wavelength. Introducing the index of refraction $n = \sqrt{\varepsilon\mu} = \sqrt{\varepsilon}$, the solution of (2) reads

$$\begin{aligned} U(z) &= A\cos(k_0 nz) + B\sin(k_0 nz)\ , \\ V(z) &= -\mathrm{i}nB\cos(k_0 nz) + \mathrm{i}nA\sin(k_0 nz)\ . \end{aligned} \tag{3}$$

The amplitudes of one layer extending from $z = 0$ to $z = z_1$ are then related by

$$\begin{aligned} Q_0 = \begin{pmatrix} U(0) \\ V(0) \end{pmatrix} &= \begin{pmatrix} \cos(k_0 nz) & -\dfrac{\mathrm{i}}{n}\sin(k_0 nz) \\ -\mathrm{i}n\sin(k_0 nz) & \cos(k_0 nz) \end{pmatrix} \begin{pmatrix} U(z) \\ V(z) \end{pmatrix} \\ &= \mathbf{M}(z)Q(z)\ . \end{aligned} \tag{4}$$

The transfer matrix $\mathbf{M}(z)$ is unimodular, i.e., its determinant is identical 1. For a stratified medium of many homogeneous layers, the total transfer matrix is obtained by multiplication of the individual transfer matrices. We consider a succession of layers extending from $0 \leqslant z \leqslant z_1$, $z_1 \leqslant z \leqslant z_2, \ldots, z_{N-1} \leqslant z \leqslant z_N$, where N is the total number of layers. For layers of thicknesses $h_i = z_i - z_{i-1}$ and refractive indices n_i, the amplitudes are then related by

$$Q_0 = \mathbf{M}_1\mathbf{M}_2\cdots\mathbf{M}_N Q_N = \mathbf{M}^{\mathrm{t}} Q_N\ , \tag{5}$$

where

$$\mathbf{M}_l = \begin{pmatrix} \cos\beta_l & -\dfrac{\mathrm{i}}{n_l}\sin\beta_l \\ -\mathrm{i}n_l\sin\beta_l & \cos\beta_l \end{pmatrix}, \quad \beta_l = k_0 n_l h_l\ , \tag{6}$$

and $\mathbf{M}^{\mathrm{t}}$ is also unimodular. Let a, r and t be the amplitudes of the incident, reflected and transmitted electric fields, respectively. The reflection coefficients R and the transmission coefficient T of the layered medium are then given by

$$\begin{aligned} R &= \frac{|r|^2}{|a|^2} = \frac{|M^{\mathrm{t}}_{11} + M^{\mathrm{t}}_{12} - M^{\mathrm{t}}_{21} - M^{\mathrm{t}}_{22}|^2}{|M^{\mathrm{t}}_{11} + M^{\mathrm{t}}_{12} + M^{\mathrm{t}}_{21} + M^{\mathrm{t}}_{22}|^2}\ , \\ T &= \frac{|t|^2}{|a|^2} = \frac{4}{|M^{\mathrm{t}}_{11} + M^{\mathrm{t}}_{12} + M^{\mathrm{t}}_{21} + M^{\mathrm{t}}_{22}|^2}\ , \end{aligned} \tag{7}$$

where $R + T = 1$. We assumed incidence from and transmission to vacuum.

Stop and transmission bands are readily identified for systems subjected to periodic (+) or antiperiodic (−) boundary conditions. According to (5), we must then have $Q_0 = \pm \mathbf{M}^t Q_0$. This means that the allowed k_0 values lead to the eigenvalue 1 of the matrix $\mathbf{M}^t$. Consequently, the condition for an allowed k_0 value is

$$\tfrac{1}{2}\mathrm{Tr}\,\mathbf{M}^t = \pm 1\,. \tag{8}$$

The condition for forbidden k_0 values is

$$\tfrac{1}{2}|\mathrm{Tr}\,\mathbf{M}^t| > 1\,. \tag{9}$$

In this case, the magnitude of one eigenvalue of $\mathbf{M}^t$ is larger than one, and the other one smaller. Accordingly, the boundary conditions are no longer satisfied. Here, we have used the fact that $\det \mathbf{M}^t = 1$; the eigenvalues of $\mathbf{M}^t$ are then given by

$$\lambda_\pm = \tfrac{1}{2}\{\mathrm{Tr}\,\mathbf{M}^t \pm \sqrt{(\mathrm{Tr}\,\mathbf{M}^t)^2 - 4}\}.$$

An alternative and for numerical studies more convenient approach to identify allowed and forbidden k_0 values is obtained in terms of recursion relations for the amplitudes Q. To derive this approach, it is useful to recall briefly the tight-binding Schrödinger problem, which reads

$$\phi_{n+1} + \phi_{n-1} = (V_n - E)\phi_n\,. \tag{10}$$

ϕ_n denotes the wave function at site n with energy E, and V_n is the respective periodic, quasiperiodic or random potential. Dividing by ϕ_n, one obtains the recursion relation[5,6])

$$R_{n+1} = V_n - E - \frac{1}{R_n}\,, \quad R_n = \frac{\phi_n}{\phi_{n-1}}\,, \tag{11}$$

which can be solved for a suitable initial value R_1. The integrated density of states $N(E)$ and the inverse exponential growth rate of the wave function $\gamma(E)$ are then given by[5,6])

$$N(E) = \frac{1}{N}\sum_{n=1}^{N}\Theta(-R_n)\,, \quad \gamma(E) = \frac{1}{N}\sum_{n=1}^{n}\ln|R_n|\,, \tag{12}$$

where $\Theta(x)$ is the unit step function. For $N \to \infty$, a gap is easily identified, because the integrated density of states $N(E)$ is constant for $E_1 \leq E \leq E_2$,

where E_1 and E_2 are the values of the band edges. In this energy region, $\gamma(E)$ is positive and vanishes at the gap edges. For energies belonging to the spectrum, $\gamma(E)$ is zero, because the associated wave function is normalizable.

In the present optical problem, an equivalent recursion relation is obtained from (4)–(6):

$$\begin{pmatrix} u_{j-1} \\ v_{j-1} \end{pmatrix} = \begin{pmatrix} \cos \beta_j & -\frac{\mathrm{i}}{n_j} \sin \beta_j \\ -\mathrm{i} n_j \sin \beta_j & \cos \beta_j \end{pmatrix} \begin{pmatrix} u_j \\ v_j \end{pmatrix} \tag{13}$$

for the amplitudes of the electric (u_j) and magnetic (v_j) fields. Eliminating v,

$$v_{j+1} = -\frac{\mathrm{i} n_{j+1}}{\sin \beta_{j+1}} (\cos \beta_{j+1} u_{j+1} - u_j) , \tag{14}$$

we find

$$u_{j+1} = \left\{ \frac{n_j \sin \beta_{j+1}}{n_{j+1} \sin \beta_j} \cos \beta_j + \cos \beta_{j+1} \right\} u_j - \frac{n_j \sin \beta_{j+1}}{n_{j+1} \sin \beta_j} u_{j-1} , \tag{15}$$

yielding the desired recursion relation

$$R_{j+1} = \frac{n_j \sin \beta_{j+1}}{n_{j+1} \sin \beta_j} \cos \beta_j + \cos \beta_{j+1} - \frac{n_j \sin \beta_{j+1}}{n_{j+1} \sin \beta_j} \frac{1}{R_j} , \tag{16}$$

where $R_j = u_j / u_{j-1}$. Thus, the optical problem has been reduced to a modified Schrödinger problem, where in addition to the potential, off-diagonal hopping matrix elements appear. The amplitude u of the electric field plays the role of the wave function, and k_0 is related to the energy. The integrated density of *states* and the inverse exponential growth rate γ can then be calculated according to (12), to identify forbidden k_0 values (*gaps*) and allowed one (*energy bands*), in analogy to the Schrödinger case. The recursion relation for the amplitudes u is also very useful since it allows the transmission coefficient T to be determined without matrix multiplications. In fact, with the initial conditions $u_0 = -v_0 = 1$, T is simply given by

$$T = \frac{4}{|u_L - v_L|^2} , \tag{17}$$

where L is the total number of layers. From this expression, one readily obtains for the well-known special case, $n_i h_i = \lambda / 4$,

$$T = \frac{4}{\left(\frac{n_2 \cdots n_{2N}}{n_1 \cdots n_{2N \pm 1}} + \frac{n_1 \cdots n_{2N \pm 1}}{n_2 \cdots n_{2N}} \right)^2} , \tag{18}$$

where the upper (+) sign holds for an odd number of layers $L = 2N + 1$, and the lower (−) sign for an even number $L = 2N$.

3. Models and numerical results

In this section, we present and interpret numerical results for multilayers consisting of two different materials denoted A and B. In solid-state lasers, the multilayer is composed of GaAs and AlAs. For these two materials, the indices of refraction are about $n_A = 3.6$ for GaAs, and $n_B = 3.0$ for AlAs, and the multilayer is fabricated by molecular-beam epitaxy, where different layers are deposited on top of one another in a very controlled fashion[8]).

Considering such a multilayer, made up from a sequence of two materials, A and B, three cases can be distinguished, (i) periodic, (ii) quasiperiodic, and (iii) random. In the periodic case, the sequence is obviously ABAB$\cdots$ABAB(A), while in the quasiperiodic case the translation rule is replaced by a non-periodic law. A familiar example is the Fibonacci inflation rule, constructed recursively as $Q_{j+1} = \{Q_j Q_{j-1}\}$ with $Q_0 = \{B\}$ and $Q_1 = \{A\}$, so that $Q_2 = \{AB\}$, $Q_3 = \{ABA\}$ and so forth. It is important to emphasize, however, that the Fibonacci inflation rule serves here merely as an example. In fact, there is an infinite number of rules to generate a sequence of elements A and B in a non-random fashion. A realization of the random case is obtained by introducing random fluctuations in the layer thickness, or in the refraction index[11,12]). From the properties of random unimodular matrices[13]), it is clear that such a random multilayer is a perfect reflector for all wavelengths when the number of layers is large enough.

In the widely used periodic case, however, both transmission and reflection occur and depend sensitively on wave number[9]). To illustrate this case, in fig. 1 we show the wave number dependence of the transmission coefficient T and the trace in terms of $x = \frac{1}{2}\mathrm{Tr}\,\mathbf{M}^t$ for a multilayer made up of 89 layers consisting of materials A and B arranged periodically, as obtained from eqs. (5)–(7). The wave number dependence is shown in terms of $\kappa = k_0 d/2\pi$, where d is the optical thickness chosen to be $d = n_A h_A = n_B h_B$. As expected from condition (8), high transmission occurs for allowed κ values where $x \sim \pm 1$. Moreover, there is a *stop band* around $\kappa = 1/4$, corresponding to the optical thickness $d = \lambda/4$. In this context, it is important to emphasize that we considered a finite periodic sequence only ($N = 89$), so that the allowed κ values do not yet form a continuous transmission band. Similarly, reflection around $\kappa = 1/4$, corresponding to the center of the stop band in the infinite sequence is still slightly smaller than 1. To provide a comparison with a corresponding multilayer composed of a very large number of layers, in fig. 2 we show the

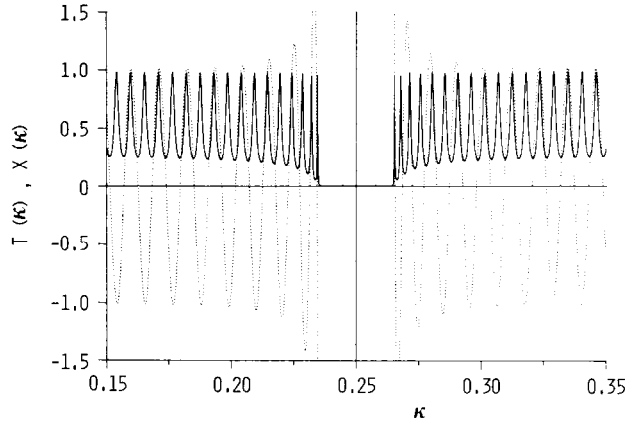

Fig. 1. Transmission T (full line) and trace x (dotted line) vs. $\kappa = k_0 d/2\pi$ for a periodic multilayer of length $N = 89$, $n_A = 3.6$, and $n_B = 3.0$ with optical thickness $d = n_A h_A = n_B h_B$. The vertical line marks $\kappa = 1/4$.

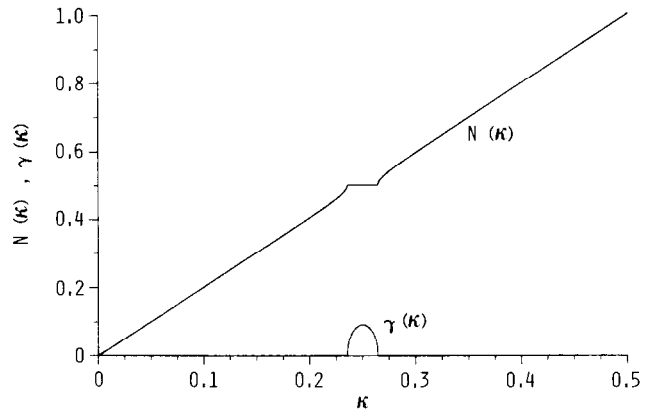

Fig. 2. Integrated density of states $N(\kappa)$, and exponential growth rate $\gamma(\kappa)$ for a periodic multilayer of length $N \sim 10^6$. The other parameters correspond to those used in fig. 1.

integrated density of states $N(\kappa)$ and the exponential growth rate $\gamma(k)$ of the associated Schrödinger problem. Here, the tendency to form a gap, corresponding to a stop band, where $\gamma(k) > 0$, and two continuous energy bands $[(\gamma(\kappa) = 0)]$ is clearly seen. For $n_A = n_B$, corresponding to one layer only, the integrated density of states reduces to $N(\kappa) = \kappa$. As seen from fig. 2, the linear κ dependence also occurs in the periodic case close to $\kappa = 0$ and $\kappa = 0.5$.

Next, we turn to the quasiperiodic case. As an example, we again consider a multilayer consisting of materials A and B and put them together according to

the Fibonacci inflation rule. This sequence is constructed as explained above, and the number of layers is given by the Fibonacci numbers

$$F_{l+1} = F_l + F_{l-1}\,, \quad F_0 = F_1 = 1\,, \tag{19}$$

where l denotes the lth Fibonacci number. We also note that

$$\lim_{l\to\infty} \frac{F_{l-1}}{F_l} = \frac{1}{\sigma_G} = \frac{\sqrt{5}-1}{2} \tag{20}$$

corresponds to the inverse golden mean. The total transfer matrix $\mathbf{M}^t$ for a sequence of length F_l, denoted by $\mathbf{M}_l$, satisfies the matrix recursion relation[3,4])

$$\mathbf{M}_{l+1} = \mathbf{M}_l \mathbf{M}_{l-1} \tag{21}$$

with initial conditions $\mathbf{M}_0 = \mathbf{M}_B$ and $\mathbf{M}_1 = \mathbf{M}_A$. In terms of the trace $x_l = \frac{1}{2}\mathrm{Tr}\,\mathbf{M}_l$, the matrix recursion relation reduces to the map[3,4])

$$x_{l+1} = 2x_l x_{l-1} - x_{l-2}\,, \tag{22}$$

with initial conditions

$$\begin{aligned} &x_0 = \cos(\beta_B)\,, \quad x_1 = \cos(\beta_A)\,, \\ &x_2 = \cos(\beta_A)\cos(\beta_B) - \eta_+ \sin(\beta_A)\sin(\beta_B)\,. \end{aligned} \tag{23}$$

This trace map has been studied in the context of the tight-binding Schrödinger problem with potential barrier heights A and B, assigned to the lattice sites[3,4,5]). It is well known and easy to check that the iteration of the trace map has an invariant

$$I(\kappa) = x_{l+1}^2 + x_l^2 + x_{l-1}^2 - 2x_{l+1}x_l x_{l-1} - 1 = \eta_-^2 \sin^2\beta_A \sin^2\beta_B\,, \tag{24}$$

where $\eta_\pm = (n_A/n_B \pm n_B/n_A)/2$. However, in contrast to the tight-binding Schrödinger model, the conserved quantity $I(\kappa)$ depends on the wave number κ. Thus, the iterates evolve on different surfaces for different wave numbers.

Fig. 3 shows the wave number dependence of transmission T and trace map x for a Fibonacci multilayer of length $F_{10} = 89$. Comparison with the periodic case, shown in fig. 1, reveals marked differences. In particular, the central *stop band* around $\kappa = 1/4$ is not present, but two stop bands appear around $\kappa \sim 0.19$ and 0.31. Moreover, outside and in between these stop bands, the transmission fluctuations are more pronounced in the quasiperiodic case. In

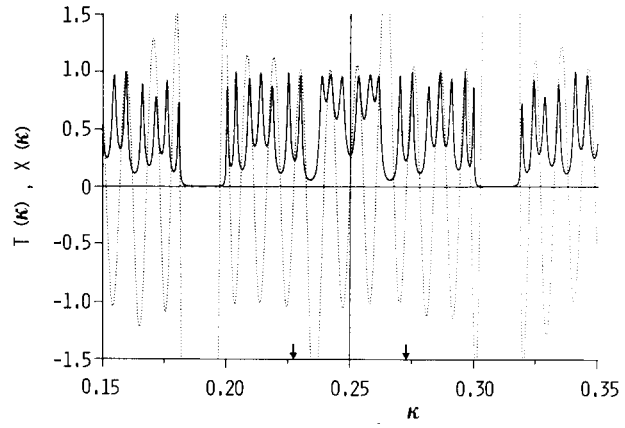

Fig. 3. Transmission T and trace x vs. $\kappa = k_0 d/2\pi$ for a Fibonacci multilayer of length $F_{10} = 89$ (effectively 68 different layers), $n_A = 3.6$ and $n_B = 3.0$ with optical thickness $d = n_A h_A = n_B h_B$. The vertical line marks $\kappa = 1/4$, and the arrows mark the interval blown up in fig. 4.

fact, about $\kappa \sim 0.236$ and 0.264 there are κ regions with very low transmission as well, becoming stop bands by increasing the number of layers. This expectation is fully confirmed by comparing figs. 3 and 4. In the larger system, with $F_{13} = 377$ layers, stop bands now appear around $\kappa \sim 0.236$ and 0.264. Comparison of figs. 3 and 4 also reveals that $T(\kappa)$ exhibits scaling properties around $\kappa = 1/4$ corresponding to $d = \lambda/4$. In fact, the behavior of $T(\kappa)$ is very similar although there is a change in the κ scale. The arrows in fig. 3 mark the κ interval blown up in fig. 4. The reason for this scaling behavior can be traced

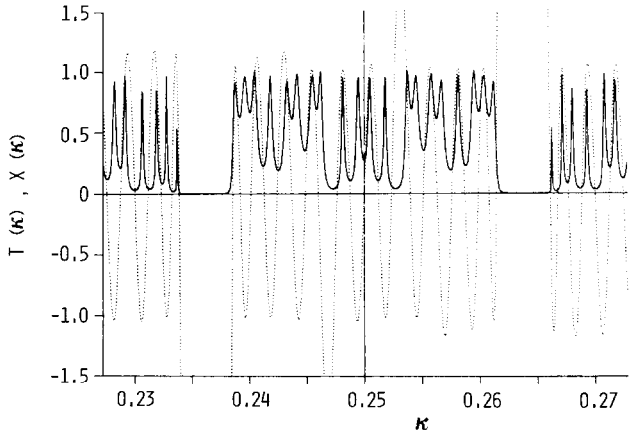

Fig. 4. Transmission T and trace x vs. $\kappa = k_0 d/2\pi$ for a Fibonacci multilayer of length $F_{13} = 377$. The other parameters correspond to those used in fig. 3.

back to the trace map (22), which for $\kappa = 1/4$ exhibits the special feature of a six-cycle, where $\beta_A = \beta_B = \pi/2$. From eqs. (22) and (23), for the amplitudes of the six-cycle we obtain $(0, 0, \eta_+, 0, 0, -\eta_+)$, and for the conserved quantity, $I = \eta_-^2$. Scaling properties then follow from the largest eigenvalue of the trace map linearized around the six-cycle and the spatial rescaling. The eigenvalues are

$$\lambda_\pm = 1 + 8\eta_+^4 \pm 4\eta_+^2\sqrt{1 + 4\eta_+^4} \,. \tag{25}$$

To illustrate the scaling property quantitatively, we turn to the integrated density of states of the associated Schrödinger equation. The numerical results as obtained from eqs. (12) and (15) are shown in fig. 5, where we also included the exponential growth rate $\gamma(\kappa)$ and the conserved quantity $I(\kappa)$. The main gaps correspond to the stop bands seen in figs. 3 and 4. The highly fragmented structure of $N(\kappa)$ and the pronounced fluctuations in the exponential growth rate $\gamma(\kappa)$ also reveal that there are gaps on all κ scales, and not merely gaps followed by bands, as in the periodic case. The highly fragmented structure of $N(\kappa)$ can be understood as follows: Gaps can be labeled by two integers n and m, positive or negative, and $N(\kappa)$ at gap n, m is given by

$$0 \leqslant n + m\sigma_G \leqslant 1 \,, \quad \sigma_G = \frac{\sqrt{5}+1}{2} \,. \tag{26}$$

This feature is also illustrated in fig. 5. As a consequence, for a very large number of multilayers there are almost only gaps. In other words, choosing κ

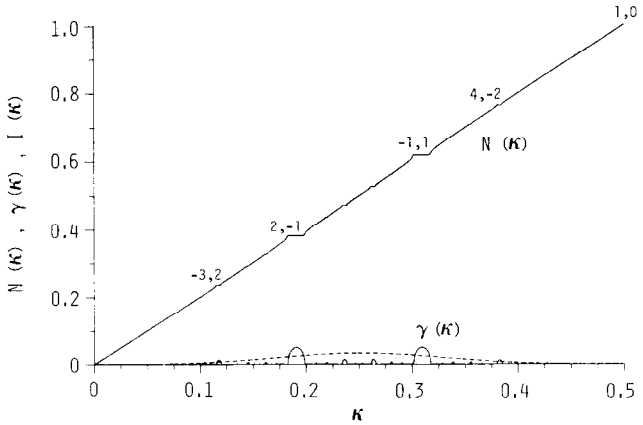

Fig. 5. Integrated density of states $N(\kappa)$, exponential growth rate $\gamma(\kappa)$ (full lines) and conserved quantity $I(\kappa)$ (dashed line) for a Fibonacci multilayer of length $N \sim 10^6$. The other parameters correspond to those used in fig. 3.

at random, κ will belong to a gap with probability one. Nevertheless, κ values with measure zero are allowed. An example is $\kappa = 1/4$ leading in the trace map to a six-cycle. Such allowed κ values yield bounded iterates, while for κ values belonging to a gap, escape occurs[3,5]).

Finally, we turn our attention to scaling properties about $\kappa = 1/4$. For the transmission, a qualitative illustration was given in figs. 3 and 4. In this context, it is important to recognize that the trace map can be derived from a recursion relation of an exact renormalization-group transformation applied to the associated Schrödinger problem[14]). Starting from a system of F_l layers, one eliminates $F_l - F_{l-1}$ to obtain an identical Schrödinger problem with renormalized parameters. One then repeats the procedure, and again eliminates $F_{l-1} - F_{l-2}$ sites to obtain a system of size F_{l-2} and so forth. This leads to recursion relations equivalent to the trace map. For an initial value κ_0 leading in the trace map to a fixed point κ^* with largest eigenvalue λ, scaling then predicts for the integrated density of states

$$|N(\kappa^* \pm \Delta\kappa) - N(\kappa^*)| = \frac{1}{\sigma_G^p} |N(\kappa^* \pm |\lambda|\Delta\kappa) - N(\kappa^*)| , \tag{27}$$

where

$$\sigma_G^p = \lim_{l\to\infty} \frac{F_{l+p}}{F_l} , \quad \sigma_G^1 = \sigma_G . \tag{28}$$

As discussed above, in the trace map $\kappa = 1/4$ leads to a six-cycle with $p = 6$. In this case, the solution of eq. (25) is

$$|N(\kappa_0 \pm \Delta\kappa) - N(\kappa_0)| \sim |\Delta\kappa|^{\bar{x}} \tag{29}$$

with

$$\bar{x} = \frac{6 \ln \sigma_G}{\ln|\lambda|} . \tag{30}$$

For $n_A = 3.6$ and $n_B = 3.0$, we then obtain $\bar{x} = 0.9895$. The estimate $\bar{x} = 0.991$, determined from the data shown in fig. 6, agrees very well. The numerical results also reveal that the scaling function exhibits periodic features. Clearly, there are many other κ values where similar scaling properties appear. For these κ values, iterates of the trace map remain bounded and include cycles with period p, aperiodic behavior or simple fixed points. Other examples are: the bottom of the spectrum, $\kappa = 0$, corresponding to fixed point $x^* = 1$, and the top, $\kappa = 0.5$, where a three-cycle $(-1, -1, 1)$ appears. Here, the scaling exponent is $\bar{x} = 1$. This value corresponds to the one-layer case where $N(\kappa) = \kappa$

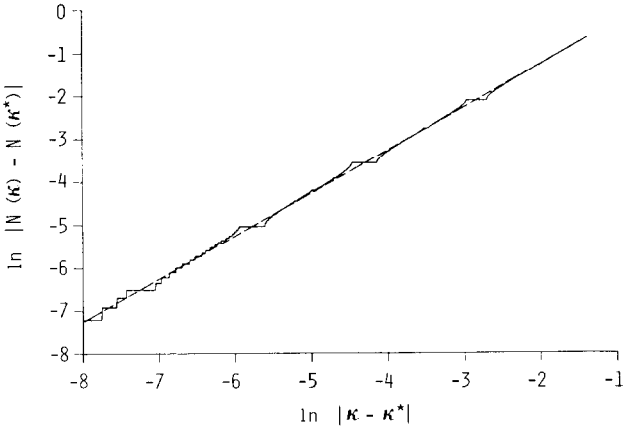

Fig. 6. Scaling behavior $\ln|N(\kappa) - N(\kappa_0)|$ vs. $\ln|\kappa - \kappa_0|$ for $\kappa_0 = 1/4$. The dashed line gives the average slope $\bar{x} = 0.9895$. The other parameters correspond to those used in fig. 3.

and $I(\kappa) = 0$. In fact, for the top and bottom $I(\kappa)$ also vanishes in the quasiperiodic case, so that the fragmented structure in $N(\kappa)$ diminishes for $\kappa \to 0$, $\to 0.5$. Thus, the degree of fragmentation becomes large where $I(\kappa)$ reaches its maximum, which increases with the ratio n_A/n_B. To illustrate these features, in fig. 7 we show the integrated density of states $N(\kappa)$, the exponential growth rate $\gamma(\kappa)$ and conserved quantity $I(\kappa)$ for $n_B = 2.0$. Comparing figs. 5 and 7, the increased degree of fragmentation accompanied by a much larger $I(\kappa)$ is clearly seen.

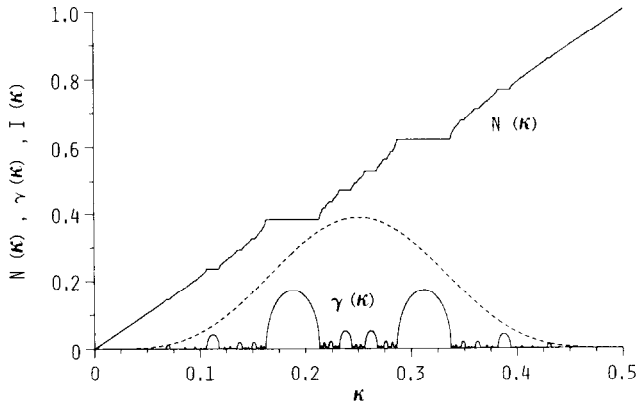

Fig. 7. Integrated density of states $N(\kappa)$, exponential growth rate $\gamma(\kappa)$ (full lines), and conserved quantity $I(\kappa)$ (dashed line) for a Fibonacci multilayer of length $N \sim 10^6$, $n_A = 3.6$, and $n_B = 2.0$ with optical thickness $d = n_A h_A = n_B h_B$.

4. Conclusions

Our results clearly reveal that quasiperiodic multilayers are in between the periodic and random cases. For sufficiently many layers, stop and transmission bands occur in the periodic case, while the random system becomes a perfect reflector at all wavelengths. In the quasiperiodic multilayer, stop and transmission bands again occur, as shown for the Fibonacci arrangement. However, their distribution is highly fragmented. This fragmentation is wave number dependent and most pronounced where the conserved quantity $I(\kappa)$ is large. It increases with the ratio $n_A/n_B > 1$, and vanishes for $n_A/n_B = 1$ where quasiperiodicity disappears. This feature offers the possibility of tailoring quasiperiodic multilayers made up according to a given inflation rule, for particular applications. Fragmentation is also a characteristic of the integrated density of states of the associated Schrödinger problem. However, it differs from the conventional case where the barrier heights form a Fibonacci sequence. Here, the fragmentation of the integrated density of states is characterized by the fractal dimension, because the conserved quantity I is energy-independent. In the optical problem, however, I depends on the wave number. As a consequence, the fragmentation is multifractal.

Acknowledgement

We should like to thank C.P. Enz, B. Movaghar and C.S. Harder for valuable discussions. One of us (MPS) thanks IBM Denmark for support.

References

1) B. Simon, Adv. Appl. Math. **3** (1982) 463.
2) J.B. Sokoloff, Phys. Rep. **126** (1985) 189.
3) M. Kohomoto, L.P. Kadanoff and C. Tang, Phys. Rev. Lett. **50** (1983) 1870.
4) S. Ostlund, R. Pandit, D. Rand, H.J. Schellnhuber and E. Siggia, Phys. Rev. Lett. **50** (1983) 1873.
5) T. Schneider, A. Politi and D. Würtz, Z. Phys. B **66** (1987) 469.
6) T. Schneider, D. Würtz, A. Politi and M. Zannetti, Phys. Rev. B **36** (1987) 1789.
7) P. Lee and T.V. Ramakrishnan, Rev. Mod. Phys. **57** (1985) 287.
8) E.H.C. Parker, The Technology and Physics of Molecular Beam Epitaxy (Plenum, New York, 1985).
9) M. Born and E. Wolf, Principles of Optics (Pergamon, London, 1959), p. 50.
10) E. Hecht and A. Zajak, Optics (Addison–Wesley, Reading, MA, 1979).
11) E. Bouchaud and M. Daoud, J. Phys. (Paris) **47** (1986) 1467.
12) C.P. Enz, Phys. Lett A **119** (1987) 432.
13) K. Ishii, Suppl. Prog. Theor. Phys. **53** (1973) 77.
14) D. Würtz, T. Schneider and A. Politi, to be published.